

Underwater propulsion using surface tension

Jessica Shang

MAE 559

8 Jan 2010

1 Introduction

While the locomotion of terrestrial snails is relatively well-understood, the locomotion of their marine counterparts is not. Terrestrial snails are able to propel themselves forward on a thin film of secreted fluid – pedal mucus – through foot contractions that propagate along the length of the foot. Pedal waves propagating in the direction of snail motion are called "direct waves"; "retrograde waves" travel in the other direction. Because the mucus is a shear-thinning fluid with a finite yield stress, shear waves caused by the foot motion results in flow near the foot, while fluid far from the foot is effectively glued to the solid substrate.

Interestingly, marine snails not only able to travel on solid substrates, but also inverted on the underside of water (see Fig. 1). The snails have been observed to employ various modes of locomotion: both retrograde and direct waves (though predominantly retrograde), swimming, and ciliary motion [1]. The kind of motion used appears to be species-dependent. However, the pedal waves of marine snails must generate traction on the underside of water in a manner different to terrestrial locomotion, since the free surface cannot support a shear stress.

To date, only one quantitative explanation has been offered for the phenomenon [1]. In the proposed mechanism, pedal waves induce deformations of the free surface, which is coupled to the topography of the snail foot. The resultant free surface is non-periodic, leading to pressure forces on the foot due to the pressure change across the curved surface. Additionally, viscous shear forces

are generated across the layer due to the traveling waves. The net propulsive force is nonzero for some values of the capillary number, even for a Newtonian mucus.

Though it is likely that marine snail mucus is non-Newtonian like their terrestrial relatives', the non-linear behavior have not been examined in the context of this particular form of locomotion. Shear-thinning fluid has been shown to be energetically favorable in terrestrial snails by minimizing the amount of fluid needed to crawl [3], so one might expect that marine snails would also benefit from a non-Newtonian mucus. In this paper, we will overview the model used by Lee et al. assuming a Newtonian fluid, expand the analysis to a non-Newtonian fluid, and compare the generated forces.



Figure 1: Snail walking on the underside of water. Credit: fotografiyfun (Flickr)

2 Motivation

Providing an explanation of how marine snails crawl on a free surface is not only of interest to biologists and fluid dynamicists, but also to roboticists. There is much current interest in applying biological principles to the design of small-scale robots. For example, robotic crawlers utilizing Newtonian or shear-thinning fluids have been constructed [2]. Outside of a biological context,

seeking the free surface shape of a fluid on a solid substrate closely resembles a coating flow on a non-planar topography.

3 Model

3.1 Description

In the analysis, a snail moves at a constant velocity \hat{V}_s by deforming its foot into n sinusoidal waves of wavelength $2\pi\hat{\lambda}$, and undulating it backwards with a known wave speed \hat{V}_w (Fig. 2(a)). (Overcarets denote dimensional variables.) In this reference frame, the shape of the foot is time-dependent, so it is more convenient to use a frame following the wave such that the foot appears fixed in time (Fig. 2(b)), so steady state governing equations may be used. Hence the geometry of the layer is described with the shape of the foot $\hat{h}_1(x)$, and the upper free surface film $\hat{h}_2(x)$.

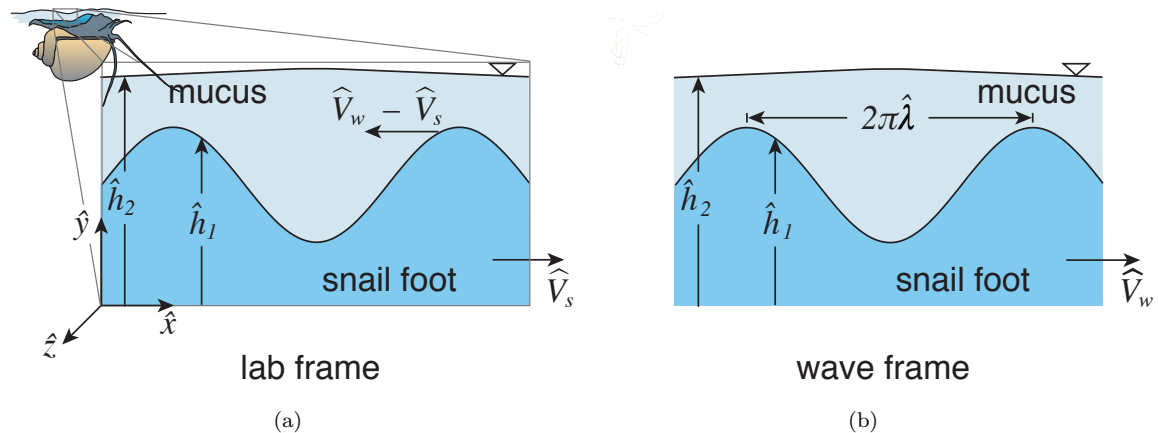


Figure 2: Cross-section of the mucus layer on the snail foot, from Lee et al. [1]. The wave speed \hat{V}_w is known (calculated relative to the snail), as is the foot shape \hat{h}_1 , and we wish to solve for the free surface \hat{h}_2 . In (a), the snail is traveling forward at \hat{V}_s ; in (b) the frame moves with the wave such that the foot shape is fixed and the snail travels forward at \hat{V}_w .

3.2 Lubrication Approximation

Assuming that the mucus velocity can be characterized by the overall snail velocity, the Reynolds number of the mucus flow is 10^{-6} , with a snail velocity of 10^{-3} m/s, a mucus thickness of $10\mu m$, density of about water, and a post-yield mucus viscosity of 10 Pa s. Furthermore, the characteristic mucus thickness \hat{H} is tens of microns thick, compared to a typical wavelength $\hat{\lambda}$ of millimeters; let this ratio be denoted by $b = \hat{H}/\hat{\lambda} \ll 1$. Hence inertial terms are ignored, and a lubrication approximation is used. Gravity can also be neglected because the snails trap air in their shells and hence are neutrally buoyant [1].

3.3 Newtonian Analysis

The lubrication equations at steady state are

$$0 = \frac{\partial \hat{u}}{\partial \hat{x}} + \frac{\partial \hat{v}}{\partial \hat{y}} \quad (1a)$$

$$0 = -\frac{\partial \hat{p}}{\partial \hat{x}} + \mu \frac{\partial^2 \hat{u}}{\partial \hat{y}^2} \quad (1b)$$

$$0 = \frac{\partial \hat{p}}{\partial \hat{y}} \quad (1c)$$

Non-dimensionalizing as follows:

$$x = \hat{x}/\hat{\lambda} \quad (2a)$$

$$y = \hat{y}/\hat{H} \quad (2b)$$

$$(u, v) = (\hat{u}, b\hat{v})/\hat{V}_w \quad (2c)$$

$$p = \hat{p}/\hat{p}_0 \quad (2d)$$

Then the lubrication equations reduce to

$$0 = \frac{\partial u}{\partial x} + \frac{\partial v}{\partial y} \quad (3a)$$

$$0 = -\frac{dp}{dx} + \frac{\partial^2 u}{\partial y^2} \quad (3b)$$

if we note that an appropriate choice for \hat{p}_0 is

$$\hat{p}_0 = \frac{\mu_0 \hat{\lambda} \hat{V}_w}{\hat{H}^2} \quad (4)$$

Integrating Eq. 3b twice with respect to y , we obtain

$$\frac{1}{2} \left[\left(\frac{dp}{dx} y + C_1(x) \right) \right]^2 \left(\frac{dp}{dx} \right)^{-1} + C_2(x) = u(x, y) \quad (5)$$

3.3.1 Boundary Conditions

The boundary conditions needed to solve the velocity is no-slip at h_1 – that is, the thin film moves at the same velocity as the wave speed of the foot \hat{V}_w . The other dictates that the upper surface is shear-free.

$$u(y = h_1) = 1 \quad (6a)$$

$$\left. \frac{\partial u}{\partial y} \right|_{y=h_2} = 0 \quad (6b)$$

Then the expression for velocity is

$$u(x, y) = 1 + \frac{1}{2} \frac{dp}{dx} [(y - h_2)^2 - (h_1 - h_2)^2] \quad (7)$$

3.3.2 Pressure

By Young-Laplace, and neglecting gravity, we can express the pressure gradient in the film as a function of the curvature of the free surface.

$$\hat{p} = -\gamma \frac{\partial^2 \hat{h}_2}{\partial \hat{x}^2} \quad (8a)$$

$$\frac{dp}{dx} = -\frac{1}{\widetilde{Ca}} \frac{\partial^3 h_2}{\partial x^3} \quad (8b)$$

if we define a "modified capillary number" as $\widetilde{Ca} = \frac{\mu \hat{V}_w}{\gamma b^3}$. Note this is not a true capillary number, as \hat{V}_w does not necessarily characterize the velocity inside the layer. Substituting this relation into Eq. 7, we obtain the velocity as

$$u(x, y) = 1 - \frac{1}{2\widetilde{Ca}} \frac{\partial^3 h_2}{\partial x^3} [(y - h_2)^2 - (h_1 - h_2)^2] \quad (9)$$

3.3.3 Solving for the Free Surface

Integrating Eq. 9 across the mucus thickness results in the volume flux through the layer¹:

$$\begin{aligned} Q &= (h_2 - h_1) + \frac{1}{2\widetilde{Ca}} \frac{\partial^3 h_2}{\partial x^3} \left(\frac{1}{3} (h_1 - h_2)^3 + (h_1 - h_2)^2 (h_2 - h_1) \right) \\ &= (h_2 - h_1) + \frac{1}{3} \frac{1}{\widetilde{Ca}} \frac{\partial^3 h_2}{\partial x^3} (h_2 - h_1)^3 \end{aligned} \quad (10)$$

The volume flux is constant because in the wave frame, the shape of the foot and the free surface are constant in time. Thus Eq. 10 is a third-order differential equation for h_2 , if a shape is prescribed for h_1 . Assuming that the foot shape is wave-like, h_1 can be expressed as

$$h_1 = \varepsilon \sin x \quad (11)$$

where $\varepsilon = \Delta \hat{H} / \hat{\lambda}$ is the size of the foot deformation. This results in a perturbation of the free surface h_2 , which can be expanded order by order as

$$h_2 = 1 + \varepsilon h_2^{(1)} + \varepsilon^2 h_2^{(2)} + O(\varepsilon^3) \quad (12)$$

¹The expression for Q (Eq. 9) in Lee et al. is incorrect, but the error surfaces as a second order effect in their perturbation analysis, and thus does not propagate through the rest of their results.

Substituting these into the expression for Q ,

$$\begin{aligned}
Q^{(0)} + \varepsilon Q^{(1)} + \varepsilon^2 Q^{(2)} = & 1 + \varepsilon(h_2^{(1)} - \sin x) + \varepsilon^2 h_2^{(2)} \\
& + \frac{a^{1/a}}{\alpha + 1} \left(\frac{1}{\widetilde{Ca}} \right)^{1/a} (\varepsilon h_{2,xxx}^{(1)} + \varepsilon^2 h_{2,xxx}^{(2)})^{1/a} \\
& (1 + \varepsilon(h_2^{(1)} - \sin x) - \varepsilon^2 h_2^{(2)})^{\alpha+1}
\end{aligned} \tag{13}$$

At zeroth order, $Q^{(0)} = 1$, but at order $O(\varepsilon)$ a linear differential equation is obtained:

$$Q^{(1)} = h_2^{(1)} - \sin x + \frac{1}{3\widetilde{Ca}} h_{2,xxx}^{(1)} \tag{14}$$

which has the solution

$$\begin{aligned}
h_2^{(1)} = Q^{(1)} & + A_1 \exp\left(-\frac{x}{C^{1/3}}\right) \\
& + A_2 \exp\left(\frac{x}{2C^{1/3}}\right) \cos\left(\frac{\sqrt{3}x}{2C^{1/3}}\right) + A_3 \exp\left(\frac{x}{2C^{1/3}}\right) \sin\left(\frac{\sqrt{3}x}{2C^{1/3}}\right) \\
& + \frac{C \cos x + \sin x}{C^2 + 1}
\end{aligned} \tag{15}$$

where $C = 1/3\widetilde{Ca}$. Three boundary conditions are required to solve for the constants. The pressure at the boundaries must match the pressure of the external flow, therefore the pressure at the head and the snail must be the same. Additionally, because the snail only moves in the x -direction, the net vertical force and the torque are zero.

$$p(0) = p(2n\pi) \tag{16a}$$

$$\sum F_y = 0 = \int_0^{2n\pi} p \, dx \tag{16b}$$

$$\sum \tau = 0 = \int_0^{2n\pi} p \, x \, dx \tag{16c}$$

where F_y is the y-force, τ is the z-torque from the thin film, and n is the number of waves along the length of the foot. This is equivalent to

$$h_{2,xx}(2n\pi) - h_{2,xx}(0) = 0 \quad (17a)$$

$$h_{2,x}(2n\pi) - h_{2,x}(0) = 0 \quad (17b)$$

$$2n\pi \ h_{2,x}(2n\pi) - h_2(2n\pi) + h_2(0) = 0 \quad (17c)$$

Therefore an expression for h_2 can be obtained to first order. A comparison of the numerical solution found by Matlab with the first-order solution for specific conditions is shown in Fig. 3. A numerical solution will be useful later in comparing the Newtonian with the non-Newtonian free surface. The analytic solution appears to be a good approximation; the deviation from the numerical solution at the head and tail are likely due to a difference in higher order terms. Though the pressure at both ends are the same, a net pressure force is still induced because the area over which the pressure is applied differs at the boundaries.

3.3.4 Propulsive Force and Snail Velocity

For a snail moving at constant velocity, the sum of the external forces around the body and the internal forces of the mucus must be zero. In the x -direction, the drag force balances the propulsive force generated by traction acting on the foot. The propulsive force can be calculated by integrating $\mathbf{\Pi} \cdot \mathbf{n_f}$ along the length of the snail, where $\mathbf{n_f}$ is the the outward normal to the foot:

$$\hat{F}_{prop} = \frac{\hat{w}\mu\hat{V}_w}{b} \int_0^{2n\pi} \left[p \frac{dh_1}{dx} + \frac{du}{dy} \Big|_{y=h_1} \right] dx \quad (18)$$

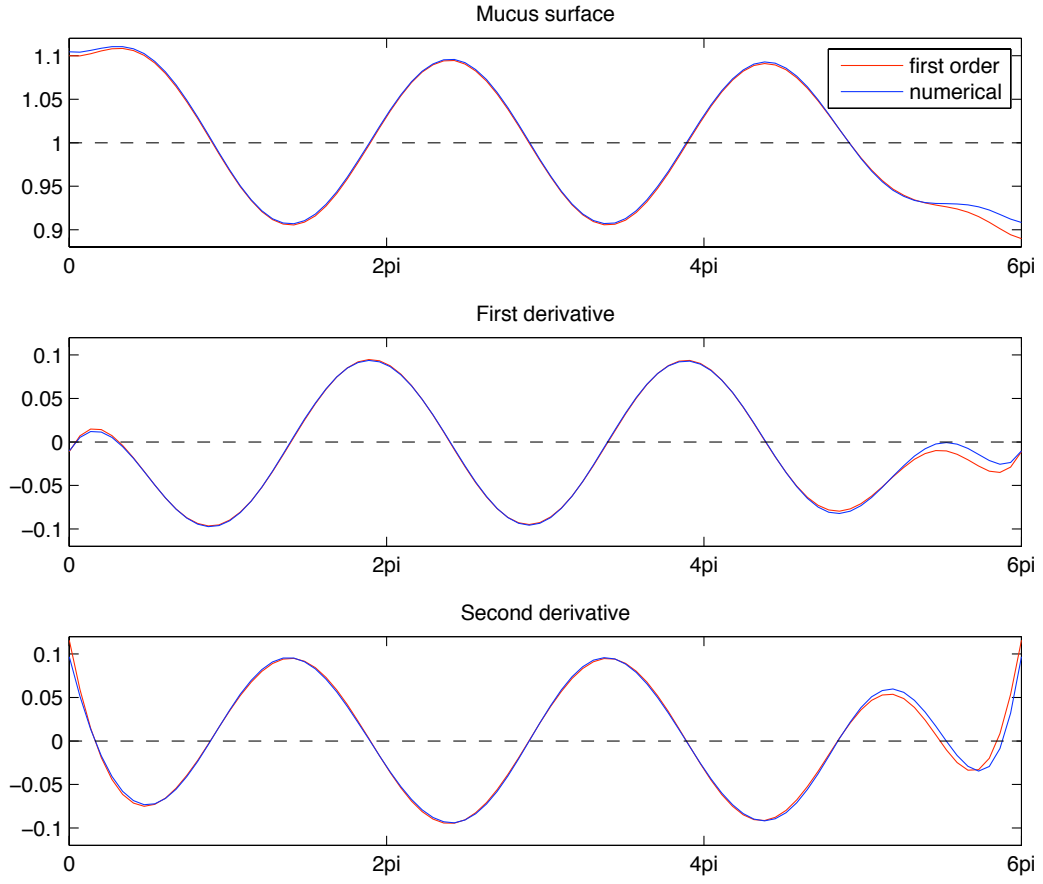


Figure 3: Comparison of the first order solution with the numerical solution, with $n = 3$ and $Ca = 1$. The dotted line marks the location of an unperturbed surface.

where \hat{w} is the width of the foot out of the page. Nondimensionalizing the force by $\frac{\hat{w}\mu\hat{V}_w}{a}$ and expressing the force only in terms of h_1 and h_2 , integration by parts yields²

$$F_{prop} = \frac{1}{\widetilde{Ca}} \int_0^{2n\pi} [-h_{2,xx}\varepsilon \cos x + h_{2,xxx}(h_2 - \varepsilon \sin x)] dx \quad (19)$$

$$= \frac{1}{\widetilde{Ca}} \left[\int_0^{2n\pi} -h_{2,xx}\varepsilon \cos x dx + h_{2,xx}(h_2 - \varepsilon \sin x) - \int_0^{2n\pi} [h_{2,xx}(h_{2,x} - \varepsilon \cos x) dx] \right] \quad (20)$$

$$= \frac{1}{\widetilde{Ca}} \left[h_{2,xx}(h_2 - \varepsilon \sin x) - \frac{h_{2,x}^2}{2} \right]_0^{2n\pi} \quad (21)$$

Applying the boundary conditions, this simplifies nicely to

$$F_{prop} = h_{2,xx}(2n\pi)(h_2(2n\pi) - h_2(0))/\widetilde{Ca} \quad (22)$$

The drag can be approximated as the viscous drag on a spheroidal object translating at a constant speed,

$$\hat{F}_{drag} = 6\pi\mu_{water}f\hat{V}_s\hat{R} \quad (23)$$

where f is a correction for the aspherical snail, and \hat{R} is the typical radius of the snail. Non-dimensionalizing and equating with Eq. 18 yields

$$V_s \approx \frac{\mu^*}{6\pi b f} F_{prop} \quad (24)$$

where μ^* is the viscosity ratio μ/μ_{water} , which is about 10^4 [4]. Thus the snail velocity is a linear function of the propulsive force.

The propulsive forces resulting from both the numerical and analytical solutions for the free surface are plotted in Fig. 4 as a function of the capillary number \widetilde{Ca} and with varying values of n . The difference between the solution is more pronounced for negative F_{prop} for unknown reasons. The forces vanish in the limit of large and small \widetilde{Ca} . When $\widetilde{Ca} \rightarrow 0$, the surface tension becomes infinitely large, and the free surface cannot be deformed. A flat surface generates no pressure

²Eq. 19 is not well-conditioned under integration, so further manipulation was necessary to obtain Eq. 22.

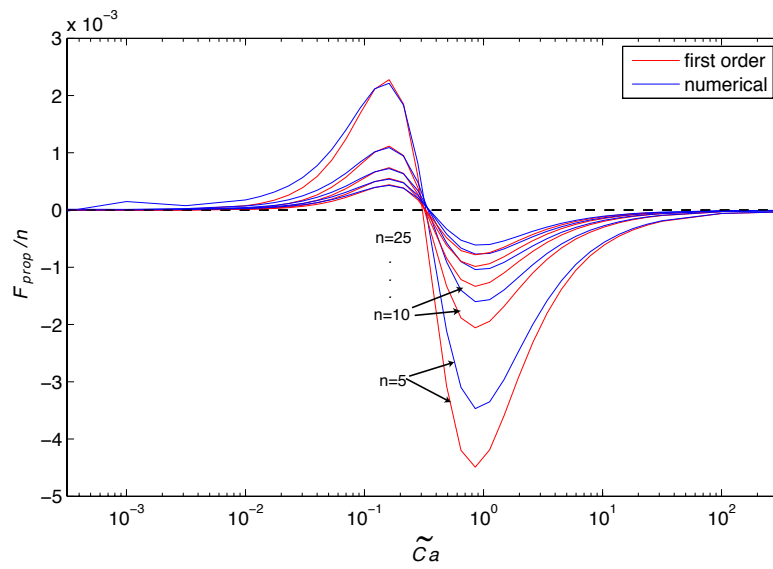


Figure 4: Comparison of the propulsive forces generated first order solution and the numerical solution, normalized per number of wavelengths.

differences across it. As $\widetilde{Ca} \rightarrow \infty$, surface tension goes to zero, so the free surface conforms to the same shape as the foot. However, there is likewise no pressure difference to drive the lubrication flow. A finite propulsive force results for intermediate \widetilde{Ca} , and equals zero at $\widetilde{Ca} \approx 0.3$, at which point the snail transitions from retrograde to direct waves.

3.3.5 Matching Mucus to Water Surface

As shown in Fig. 3, the mucus layer deviates from the flat surface at the snail's head and tail. Additional capillary forces arise from the curvature resulting from matching the mucus layer to the far-field flat surface. The force analysis in the previous section will only hold in the limit that the intermediate forces can be ignored.

The size of the intermediate region is characterized by either \hat{w} or \hat{l}_c , the capillary length. Larger capillary forces are generated by the smaller length, as the matching curvature will be greater. For most snails \hat{l}_c will be smaller; for $\gamma \sim 10^{-3}$ N/m [1], this is about 0.3 mm. The pressure across this curvature is $\sim \gamma \delta \hat{h} / \hat{l}_c^2$, where $\delta \hat{h}$ is the typical height of the surface distortion. The capillary force per unit width applied over a height $\delta \hat{h}$ is

$$\hat{F}_{cap} \sim \gamma \delta \hat{h}^2 / \hat{l}_c^2 \sim \gamma \varepsilon^2 b^2 \hat{\lambda}^2 / \hat{l}_c^2 \quad (25)$$

noting that the typical \hat{h} is on the same order as the foot deformation. This must match the external force per unit width, which is the viscous drag $\sim \mu \hat{V}_s$. $\hat{V}_s \sim \hat{F}_{prop} \sim \varepsilon^2 \hat{V}_w$, since \hat{F}_{prop} is a function of two quantities of magnitude ε (Eq. 22). Then the matching condition becomes

$$\gamma \varepsilon^2 b^2 \hat{\lambda}^2 / \hat{l}_c^2 \ll \varepsilon^2 \mu \hat{V}_w \quad (26)$$

or equivalently

$$\hat{R}^2 / \hat{l}_c^2 \ll b \widetilde{Ca} n^2 \quad (27)$$

where $\hat{R} \sim n \hat{\lambda}$ is approximately the length of the snail. Thus n must be sufficiently large. For a 1cm-long snail with $b \sim 10^{-2}$ [1], 10 or fewer waves is sufficient to fulfill this condition for

$$\widetilde{Ca} > 10^{-2}.$$

3.4 Shear-Thinning Fluid

The mucus secreted by terrestrial snails is a shear-thinning fluid, and it has been shown that this is energetically favorable compared to a Newtonian fluid [3]. Because marine snails similarly crawl on solid substrates, marine snail mucus probably has similar properties. Though we have demonstrated above that a Newtonian fluid with finite surface tension is sufficient to generate propulsive forces, it would be interesting to whether or not a non-Newtonian mucus would have a significant effect.

For a non-Newtonian fluid in Stokes' flow, we must begin with the conservation of momentum:

$$\hat{\nabla} \hat{p} = \hat{\nabla} \cdot \hat{\tau} \quad (28)$$

where \hat{p} is the pressure and $\hat{\tau}$ is the deviatoric stress tensor (the stress tensor $\mathbf{\Pi}$ minus the pressure part). In the manner of Chan et al., the fluid mucus is modeled as a Herschel-Bulkley fluid:

$$|\hat{\tau}| \geq \tau_0 : \quad |\hat{\tau}| = (\tau_0 + \mu |\dot{\sigma}|^a) \text{sgn}(\dot{\sigma}) \quad (29)$$

$$|\hat{\tau}| < \tau_0 : \quad \frac{\partial \hat{u}}{\partial \hat{y}} = 0 \quad (30)$$

where $\hat{\tau}$ is the xy component of the deviatoric stress tensor, τ_0 is the yield stress, μ is the consistency, $\dot{\sigma} = \frac{\partial \hat{u}}{\partial \hat{y}}$ is the strain rate, and a is the power law index. Non-dimensionalizing as follows:

$$x = \hat{x} / \hat{\lambda} \quad (31a)$$

$$y = \hat{y} / \hat{H} \quad (31b)$$

$$u = \hat{u} \frac{1}{\hat{H}} \frac{a}{a+1} \left(\frac{\mu}{2\tau_0} \right)^{1/a} \quad (31c)$$

$$p = b\hat{p} / \tau_0 \quad (31d)$$

conveniently transforms the lubrication equations as

$$|\tau| \geq \tau_0 : \quad \frac{\partial p}{\partial x} = \frac{\partial}{\partial y} \left[\left(1 + 2 \left| \frac{a}{a+1} \frac{\partial u}{\partial y} \right|^a \right) \text{sgn}(\dot{\sigma}) \right] \quad (32)$$

$$|\tau| < \tau_0 : \quad \frac{\partial u}{\partial y} = 0 \quad (33)$$

3.4.1 Boundary Conditions

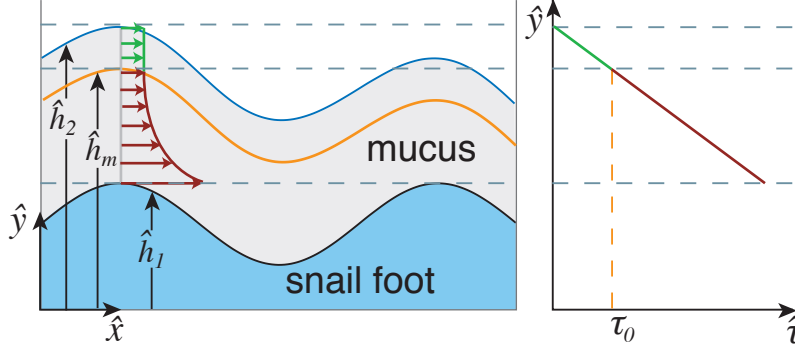


Figure 5: For a mucus with a finite yield stress, the flow through the layer is divided into two regions, meeting at the orange line \hat{h}_m . In the bottom region, the fluid is sheared, while the top region is shear-free. To the right is a plot of \hat{y} versus the xy component of the deviatoric stress tensor.

There are two flow regions – flow next to the foot, where the fluid experiences shear from the moving boundary and is above the yield stress, and flow next to the free surface that is shear-free, since the stress is below the yield stress (Fig. 5). These two regions meet at some intermediate height h_m . Velocity is continuous across h_m and smooth, such that $\frac{\partial u}{\partial y} \Big|_{y=h_m} = 0$. Imposing no-slip at h_1 and these boundary conditions, and knowing that $\text{sgn}(\dot{\sigma}) = -1$ in the bottom region, we can solve for the velocity as

$$u_1(x, y) = 1 + \left(\frac{1}{2} \frac{dp}{dx} \right)^{1/a} \left[(h_m - y)^{1/a+1} - (h_m - h_1)^{1/a+1} \right] \quad (34)$$

In the top region, u_2 is constant in y . By matching, u_2 is equal to the velocity at the top of the

bottom region:

$$u_2(x) = 1 - \left(\frac{1}{2} \frac{dp}{dx} \right)^{1/a} (h_m - h_1)^{1/a+1} \quad (35)$$

3.4.2 Pressure

By Young-Laplace,

$$\mathbf{n} \cdot \mathbf{\Pi} \cdot \mathbf{n} = \gamma \kappa \quad (36)$$

where κ is the free surface curvature and \mathbf{n} is the normal to the free surface. The stress tensor $\mathbf{\Pi}$ differs from the Newtonian case, but because we are concerned with the stress tensor evaluated at the free surface, the expression for pressure is still the same (Eq. 8a, 8b), if we define a new \widetilde{Ca} as $\widetilde{Ca} = \tau_0 \hat{\lambda} / (b^2 \gamma)$. Though this is not the same as the Newtonian \widetilde{Ca} , the yield stress τ_0 is probably of the same order as $\mu \hat{V}_w / \hat{H}$.

3.4.3 Solving for the Free Surface

As in the Newtonian case, the mass flux at any position x is constant. Integrating across y in the respective regions yields

$$\begin{aligned} Q &= \int_{h_1}^{h_m} u_1(x, y) dy + (h_2 - h_m) u_2(x) \\ &= h_2 - h_1 - \left(\frac{1}{2} \frac{dp}{dx} \right)^{1/a} \left((h_m - h_1)^{1/a+1} (h_2 - y_m) + \frac{a+1}{2a+1} (h_m - h_1)^{1/a+2} \right) \end{aligned} \quad (37)$$

where h_2 and h_m are unknowns. However, since $\hat{\tau}$ linearly decreases with y with a slope $d\hat{p}/d\hat{x}$, we note that there is a yield condition

$$\frac{d\hat{p}}{d\hat{x}} = \frac{\tau_0}{\hat{h}_2 - \hat{h}_m} \quad (38)$$

which, when non-dimensionalized, can be substituted into Eq. 37 for h_m to obtain a differential equation for h_2 . However, this is a particularly tedious equation, and not easy for a numerical solver, so let us consider two limits of the yield stress. In one scenario, the yield stress is high, and

hence the no-shear layer is thin. Taking the limit as $h_m \rightarrow h_2$ yields

$$Q = (h_2 - h_1) - \frac{a+1}{2a+1} \left(-\frac{1}{2\widetilde{C}a} h_{2,xxx} \right)^{1/a} (h_2 - h_1)^{1/a+2} \quad (39)$$

In the other limit $h_m \rightarrow h_1$, as yield stress is low resulting in a thick no-shear layer,

$$Q = h_2 - h_1 \quad (40)$$

In the latter case, the shape of the mucus layer exactly conforms to the shape of the foot. Again assuming a sinusoidal foot shape, we can obtain the propulsive force³ as

$$F_{prop} = \frac{\varepsilon}{\widetilde{C}a} \int_0^{2n\pi} (\varepsilon \sin x \cos x - \cos x) dx = 0 \quad (41)$$

which we could have guessed because the pressure at the head and the tail are the same, and the area over which the mucus acts as well, resulting in no net force. Thus we can see that the no-shear layer does not contribute to the net propulsive force generated by the snail. Henceforth we will consider the other limit in which the flow is always post-yield, thus maximizing the propulsive force.

Examining Eq. 39, it is impossible to similarly solve the differential equation in the same manner as with a Newtonian fluid, because we cannot collect like order terms when $a \neq 1$, as the powers of ε can be non-integral. Instead, h_2 was solved numerically with Matlab's bvp4c solver, using between 4000 and 8000 mesh points. With decreasing a the solver was increasingly unable to achieve the desired accuracy, but the solution is still a good estimate.

³I originally solved this non-Newtonian force with Eq. 18, but I belatedly realize that this may not be wholly correct, as the x-component of $\mathbf{\Pi} \cdot \mathbf{n}$ is not the same. The propulsive force really should be

$$\begin{aligned} \hat{F}_{prop} &= \hat{w} \int \hat{p} \hat{h}_{1,\hat{x}} + (\tau_0 + \mu |\dot{\sigma}|^a) \text{sgn}(\dot{\sigma}) d\hat{x} \\ &= \hat{\lambda} \hat{\tau}_0 \hat{w} \int_0^{2n\pi} p h_{1,x} + (1 + 2 \left| \frac{n}{n+1} \frac{\partial u}{\partial y} \right|^a) \text{sgn}(\dot{\sigma}) dx \\ &= \hat{\lambda} \hat{\tau}_0 \hat{w} \int_0^{2n\pi} p h_{1,x} - 1 - \frac{dp}{dx} (h_m - h_1) dx \end{aligned}$$

which doesn't make sense because the "1" term results in a very large force, especially as n increases.

3.5 Non-Newtonian Effects

An illustrative comparison between the foot shape generated by Newtonian and non-Newtonian mucus is given in Fig. 6. Qualitatively, the shapes are similar, though the amplitude is larger for decreasing a . This is unsurprising; a shear-thinning fluid will flow more readily, leading to larger perturbations in the free surface.

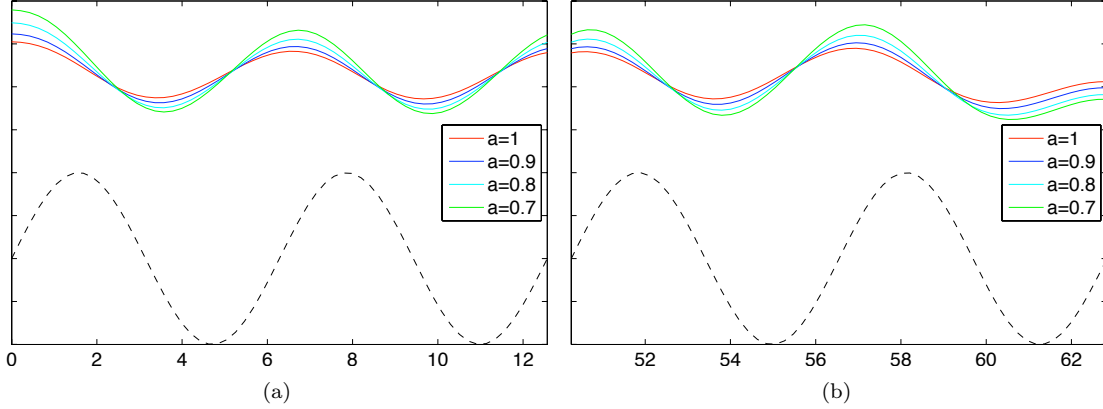


Figure 6: Shape of the free surface at the front (a) and back (b) of the snail at $\widetilde{Ca} = 0.1$ and $n = 10$ varying the power law index, where $a = 1$ corresponds to a Newtonian fluid. The black dashed curve illustrates the foot shape.

Because of the larger disturbances, a greater asymmetry in thickness exists at the head and tail, leading to a greater propulsive force. This is confirmed in Fig. 7, where increased thinning leads to greater forces. Decreasing the power law index is also accompanied by a negative shift in the retrograde-direct wave transition \widetilde{Ca} , and the locations of \widetilde{Ca} that produce the maximum retrograde or propulsive forces. Thus a snail that uses a more shear-thinning fluid limits the \widetilde{Ca} regime in which it can use retrograde waves, and the payoff for using direct waves is much greater with a shear-thinning fluid, which is at odds with observations that marine snails largely use retrograde pedal waves [2].

In both Newtonian and non-Newtonian cases, the maximum or minimum F_{prop} appears to approach an asymptotic value as n becomes large (Fig. 8). However, this force is only slightly

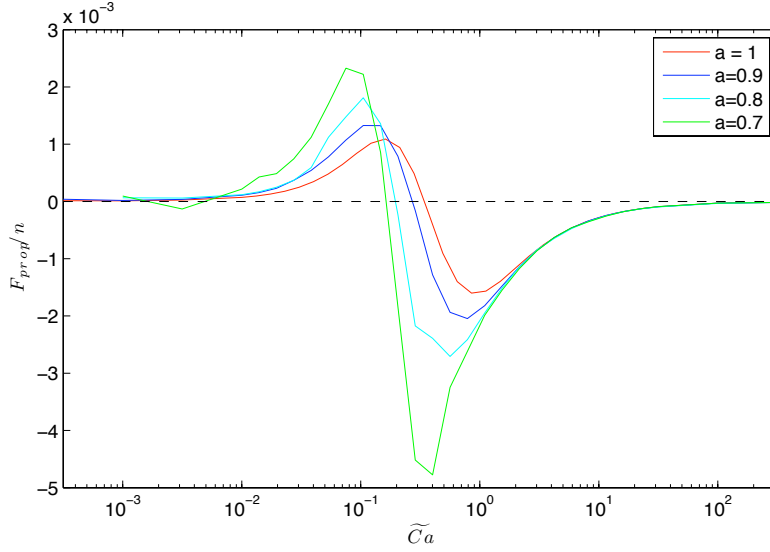


Figure 7: Comparison of the Newtonian and shear-thinning propulsive forces, normalized by the number of waves ($=10$). Some of the data appear irregular, due to issues with the numerical solver being unable to meet the specified tolerance with the number of mesh points allowed.

larger than if using just a few waves, which energetically costs less, and as we have previously asserted, few waves are necessary to ensure matching of the mucus to the free interface (Eq. 27).

4 Concluding Remarks

We have demonstrated that surface tension is a viable mechanism by which a snail can generate propulsive forces on a free surface, as long as the surface tension is not very small or very large. Expanding on the Newtonian model presented by Lee et al., a shear-thinning fluid is shown to significantly increase these propulsive forces as nonlinearity increases. As the fluid is more receptive to deformation, surface perturbations are exaggerated, leading to greater forces. However, the model suggests that direct waves are advantageous over retrograde waves, though retrograde is more commonly observed in marine snails. Therefore, it would be valuable if the model could be experimentally validated with a particular snail species. Using available data in the literature [1][4],

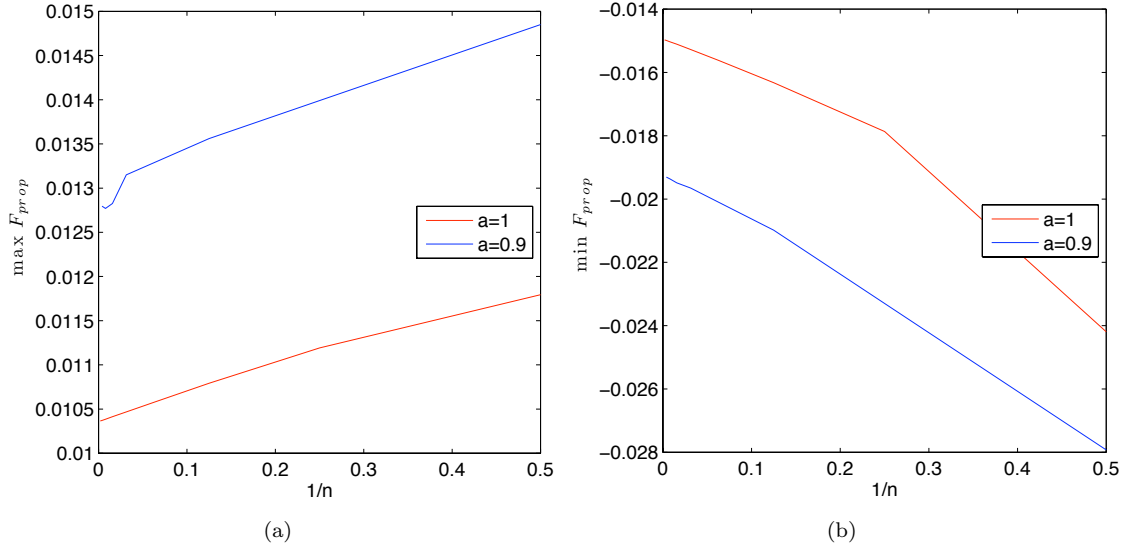


Figure 8: Maximum (a) and minimum (b) propulsive forces as a function of n^{-1} for both a Newtonian and non-Newtonian fluid.

some typical values are

$$\begin{aligned}
 \mu &\sim 10 \text{ Pa s} \\
 \gamma &\sim 10^{-3} \text{ N/m} \\
 \hat{\lambda} &\sim 1 \text{ mm} \\
 b &\sim 10^{-2}
 \end{aligned}$$

generating a \widetilde{Ca} of $10^{10} \hat{V}_w$ for a Newtonian fluid. To be in agreement with the model, a significant propulsive force would be generated for a wave speed of $\sim 10^{-9}$ to 10^{-12} m/s, which corresponds to a snail speed of $\sim 10^{-5}$ to 10^{-8} m/s. This is much slower than observed speeds of 1 mm/s. Using a yield stress of 10^2 Pa [4], we obtain a non-Newtonian \widetilde{Ca} of 10^6 ; by the described model, this generates no propulsive force. Clearly there is an incongruity within the set of values used and with the model. A complete set of typical values would shed light on whether or not pedal wave-induced surface deformation is actually a significant source of propulsive force. In one set of

experiments, snails continued to move even when a high concentration of surfactant was applied to the foot, greatly decreasing the surface tension and perhaps indicating a greater role of other modes of locomotion, such as ciliary motion [5]. Alternatively, a device similar to the snail crawler could be constructed to test the hypothesis, though it may have to be conducted in a denser medium to ensure neutral buoyancy [2].

References

- [1] S. Lee, J. W. M. Bush, A. E. Hosoi, and E. Lauga, “Crawling beneath the free surface: Water snail locomotion,” *Phys. Fluids*, **20**, 08216 (2008).
- [2] B. Chan, N. J. Balmforth, A. E. Hosoi, “Building a better snail: Lubrication and adhesive locomotion,” *Phys. Fluids*, **18**, 113101 (2005).
- [3] E. Lauga and A. E. Hosoi, “Tuning gastropod locomotion: Modeling the influence of mucus rheology on the cost of crawling,” *Phys. Fluids*, **18**, 113102 (2006).
- [4] R. H. Ewoldt, C. Clasen, A. E. Hosoi, and G. H. McKinley, “Rheological fingerprinting of gastropod pedal mucus and synthetic complex fluids for biomimicking adhesive locomotion,” *Soft Matter* **3**, 634 (2007).
- [5] K. Aono, A. Fusada, Y. Fusada, W. Ishii, Y. Kanya, M. Komuro, K. Matsui, S. Meguro, A. Miyamae, Y. Miyamae, A. Murata, S. Narita, H. Nozaka, W. Saito, A. Watanabe, K. Nishikata, A. Kanazawa, Y. Fujito, M. Yamagishi, T. Abe, M. Nagayama, T. Uchida, K. Gohara, K. Lukowiak, and E. Ito. “Upside-Down Gliding of *Lymnaea*,” *Biol. Bull.*, **215**, 272-279 (2008).